

A Feasibility Study for Passive Load-Follow Operation of Micro Molten Salt Reactor with Dynamics of Delayed Neutron Precursor

Youngjune Lee^{a*}, Taesuk Oh^a, Eunhyug Lee^a, and Yonghee Kim^{a*}

^aDepartment of Nuclear & Quantum Engineering, Korea Advanced Institute of Science and Technology (KAIST),
291 Daehak-ro, Yuseong-gu, Daejeon 34141, Republic of Korea

*Corresponding author: yongheekim@kaist.ac.kr

***Keywords:** Molten Salt Reactor (MSR), Passive Load-Follow Operation (PLFO), Delayed Neutron Precursor (DNP)

1. Introduction

In the realm of innovative GEN IV reactor, Molten Salt Reactor (MSR) stands out as a promising design for micro application owing to its remarkably simple system where fuel and coolant are integrated in the primary loop and the superior inherent safety coming from the strongly negative fuel temperature coefficient.

Driven by the demand for active contribution to local microgrid such as shoreline, village or remote area, the concept of passive load-follow operation (PLFO) has emerged to improve power maneuvering capacity and autonomy, thereby minimizing reliance on active control mechanisms.

Despite the Micro MSR's advantageous neutronic properties for PLFO, the distinctive dynamics stemming from the circulating liquid fuel system necessitate meticulous integration into kinetic models. Consequently, a feasibility study on PLFO for Micro MSR has been conducted, incorporating the influence of drifting delayed neutron precursors (DNPs) on reactivity, within a simplified thermal-hydraulic (TH) model framework.

2. Conceptual Design of Micro MSR

2.1 Conceptual Design and Kinetic Parameters

The shape of the active core is simple cylindrical structure with a wedge-shaped structure in the bottom side, to facilitate the fuel salt flow. The overall core configuration, encompassing reflectors, control drums, inlet/outlet pipes, etc., is illustrated in Figs. 1 and 2.

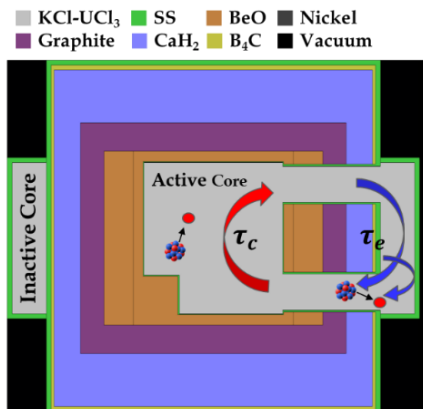


Fig. 1. Side view of Micro MSR

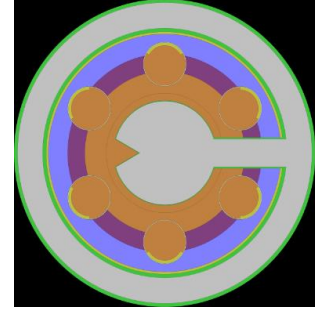


Fig. 2. Top view of Micro MSR

Table I depicts the nominal design parameters of Micro MSR. The nominal core inlet and outlet temperatures are computed using the heat transport equation, Eq. (4), assuming a nominal fuel average temperature of 635°C. The specific heat of KCl-UCl₃ is assumed constant, which corresponds to the computed value with 54-46 mole fraction and temperature range of interest. [1] The residence times of delayed neutron precursors in the active and inactive cores are determined using Eqs. (1) and (2), where M_c and M_e denote the mass of fuel salt in the active and inactive core, respectively.

$$(1) \tau_c = \frac{M_c}{w(t)}$$

$$(2) \tau_e = \frac{M_e}{w(t)}$$

The transit times of the hot leg and cold leg, which is a portion of the inactive core residence time, are derived using Eq. (3), with M_{HX} denoting the mass of fuel salt flowing in the heat exchanger.

$$(3) \tau_c = \frac{M_e - M_{HX}}{2.0 * w(t)}$$

Table I: Nominal design parameters of Micro MSR

Nominal thermal power [MW _{th}]	7.0
Mass of fuel salt in the active core [kg]	1225.3
Mass of fuel salt in the inactive core [kg]	3014.71
Fuel salt flowing in the heat exchanger [kg]	2174.71
Specific heat of fuel salt, C_p [J kg ⁻¹ K ⁻¹]	475
Salt flow rate in the primary loop [kg s ⁻¹]	420
Nominal core inlet temperature [°C]	619.96
Nominal core outlet temperature [°C]	650.04
Nominal core average temperature [°C]	635

Secondary salt temperature [°C]	535
Active core residence time, τ_c [s]	2.9174
Inactive core residence time, τ_e [s]	7.1779
Hot leg transit time, τ_{dh} [s]	1.0
Cold leg transit time, τ_{dc} [s]	1.0
Fuel temperature coefficient, α_f [pcm K ⁻¹]	-6.14
Reflector temperature coefficient [pcm K ⁻¹]	3.31
Prompt neutron generation time [s]	9.8E-05

Neutronic and kinetic parameters are computed under reactor isothermal conditions with 635°C at beginning of life (BOL), using Monte Carlo-based reactor criticality calculation code Serpent 2.2.0 and ENDF/B-VII.1 library. Temperature feedback coefficients are evaluated across temperature ranges of 535-635°C and 635-735°C. Table II details the adjoint-weighted effective delayed neutron fraction and decay constants for each of the six groups of delayed neutron precursors.

Table II: Kinetic parameters of Micro MSR

Group	β_i [pcm]	λ_i [s ⁻¹]
1	22.78	1.336E-02
2	121.32	3.257E-02
3	116.84	1.211E-01
4	275.42	3.064E-01
5	126.54	8.636E-01
6	51.82	2.901E+00
Total	714.72	5.074E-01

2.2 Simplified Primary Loop and Heat Exchanger

Fig. 3 illustrates the schematic diagram of the simplified analysis model, integrating a 1-D reactor and heat exchanger, accounting for delayed transit time. The temperature of the secondary salt loop (T_{IC}) is assumed to be constant at 535°C, 100°C lower than the nominal fuel average temperature. In this scheme, the inlet and outlet temperatures of the core and heat exchanger are represented as specified below.

$$(4) T_{HX}^{in}(t) = T_f^{out}(t - \tau_{dh})$$

$$(5) T_f^{in}(t) = T_{HX}^{out}(t - \tau_{dc})$$

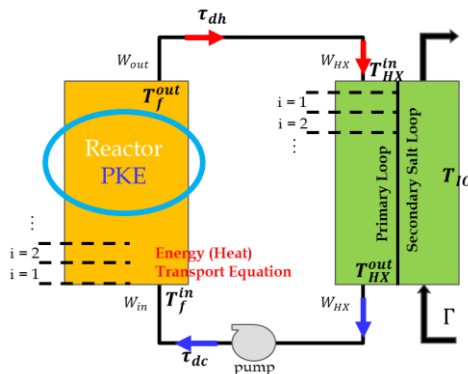


Fig. 3. Scheme of simplified analysis model

3. System Modeling and Results

3.1 Point Kinetics Equation in the circulating fuel system

To incorporate the effect of circulating delayed neutron precursors (DNPs) on reactivity, conventional Point Kinetics Equations are modified with additional terms accounting for DNP dynamics. [2] In the RHS of Eq. (7), third and fourth term represents the rate of DNP each drifting from the active core and re-entering the active core after decaying in the inactive core. Implicit Euler scheme was utilized with a time step of 10⁻⁴ s.

$$(6) \frac{dP(t)}{dt} = \frac{\rho(t) - \beta}{\Lambda} P(t) + \sum_{i=1}^6 \lambda_i C_i(t)$$

$$(7) \frac{dC_i(t)}{dt} = \frac{\beta_i}{\Lambda} P(t) - \lambda_i C_i(t) - \frac{C_i(t)}{\tau_c(t)} + \frac{C_i(t - \tau_e) \exp(-\lambda_i \tau_e)}{\tau_c(t)} \quad \text{for } i = 1, \dots, 6$$

By imposing the steady-state conditions for Eqs. (6) and (7), the loss of DNPs can be quantified, as detailed in Eq. (8), highlighting the initial necessity of additional reactivity (ρ_0) to maintain the reactor at a steady-state. The loss of DNPs at constant nominal flow rate are enumerated in Table III. For the DNPs with longer half-life, the loss tends to converge to the ratio of the inactive core volume to the whole core volume, 0.71.

$$(8) \rho_0 = \beta - \sum_{i=1}^6 \frac{\beta_i \lambda_i}{\lambda_i + 1/\tau_c(1 - \exp(-\lambda_i \tau_e))}$$

Table III: Loss of DNP of each 6 group [pcm] and [% loss]

1G	2G	3G	4G	5G	6G	Total
16.0	83.3	72.6	137	35.9	5.48	351
70 %	69 %	62 %	50 %	28 %	11 %	49 %

3.2 1-D Thermal-Hydraulics scheme

For time-varying power scenarios, a 1-D energy (heat) transport equation is adopted to the active core, incorporating the fission power distribution (f^i) from the initial steady state as given in Eq. (9). [2] A similar 1-D TH model is applied to the heat exchanger, condensed into a single node as given in Eq. (10), with Γ representing the mass flow rate of the secondary salt.

$$(9) \frac{dT_f^i(t)}{dt} = \frac{f^i}{M^i C_p} P(t) + \frac{W(t)}{M^i} (T_f^{i-1}(t) - T_f^i(t))$$

for $i = 1, \dots, N_c$

$$(10) \frac{dT_{HX}^{Pr}(t)}{dt} = \frac{W(t)}{M_{HX} C_p} (T_{HX}^{in}(t) - T_{HX}^{out}(t)) + h_{ic} A_{ic} \Gamma (T_{IC} - T_{HX}^{Pr}(t))$$

$$(11) T_{HX}^{Pr} = \frac{T_{HX}^{in}(t) + T_{HX}^{out}(t)}{2}$$

The reactivity feedback from fuel temperature variation, involving Doppler and fuel salt density effects

from the fuel temperature coefficient, is represented in Eq. (12). Total reactivity is expressed as Eq. (13), the sum of DNPs loss and feedback from fuel temperature.

$$(12) \quad \rho_f(t) = \alpha_f(T_f^{avg}(t) - T_f^{nominal})$$

$$(13) \quad \rho(t) = \rho_0(t) + \rho_f(t)$$

To ensure the feasibility of PLFO, it is imperative that the temperature feedback remains clearly negative. Although the reflector temperature feedback coefficient is positive, focusing solely on the fuel temperature feedback effect suffices for preliminary PLFO simulations of the MSR since the temperature change of the reflector region in this MSFR structure is negligible compared to the circulating fuel salt. This is attributable to the distinct separation between the active core and the bulky reflectors which are loaded in the out-of-core part.

3.3 PLFO simulation for quickly varying power demand

PLFO simulations, adjusting the secondary salt flow rate (Γ) according to power demand, have been executed under both quickly and slowly varying power demands. Two cases of pump speed are subordinately considered: one with a constant pump speed, corresponding to the nominal fuel salt flow rate of 420 kg/s, and another with an adaptive pump speed, proportionally adjusted by power demand as given in Eq. (14). In this case, $w(t)$ is reflected to Eqs. (1-13) at every time step. This implies that active reactivity control, such as revolving control drum, is being induced to counteract varying reactivity loss from drifting DNPs according to Eq. (8).

$$(14) \quad w(t) = 420 * \frac{\Gamma}{\Gamma_0} [kg/s]$$

Reactivity in Figs. 5 and 7 means the fuel temperature feedback reactivity which corresponds to the difference between total reactivity and beta loss in Figs. 4 and 9.

In quickly varying power demand simulations, Γ is adjusted with the speed of 10 % level per 15 s. Both case A and B successfully followed the quickly varying load in overall behavior, with some time delay. Case A, employing a fixed pump speed, exhibits larger variations in core inlet and outlet temperatures from nominal state compared to Case B, resulting in a slight power demand overshoot as shown in Fig. 5. Case B exhibits a slight undershoot of the local peak as shown in Fig. 7.

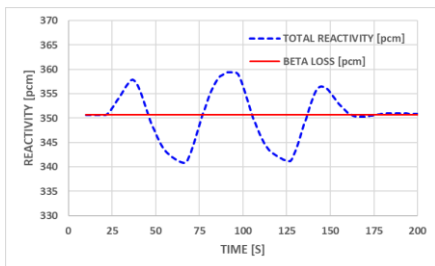


Fig. 4. Reactivity profile with constant pump speed (A)

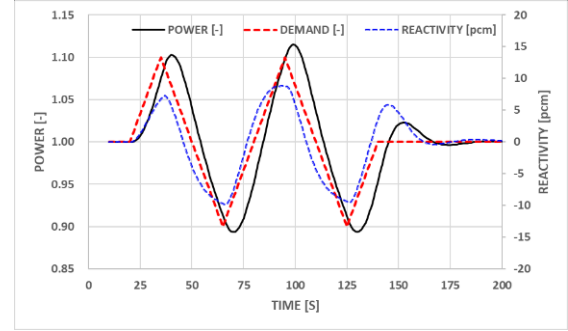


Fig. 5. Power profile with constant pump speed (A)

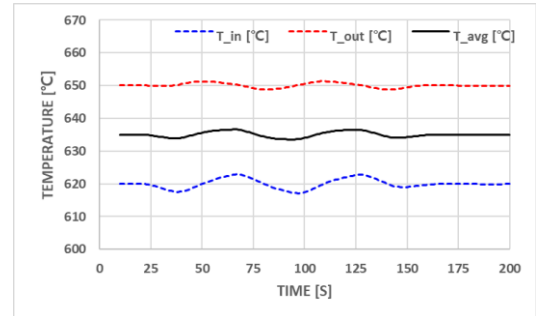


Fig. 6. Temperature profile with constant pump speed (A)

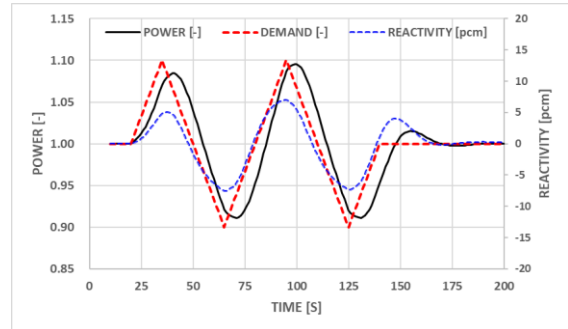


Fig. 7. Power profile with adaptive pump speed (B)

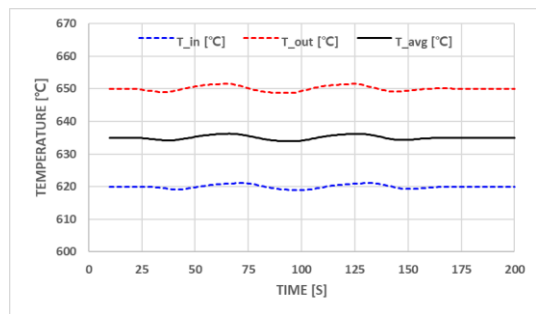


Fig. 8. Temperature profile with constant pump speed (B)

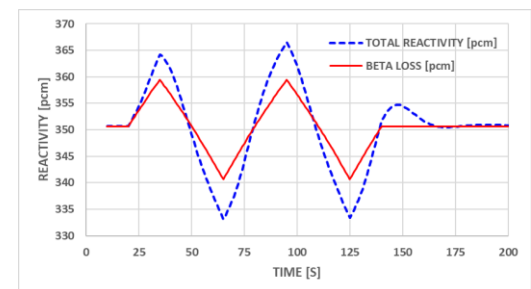


Fig. 9. Reactivity profile with adaptive pump speed (B)

3.4 PLFO simulation for slowly varying power demand

In slowly varying power demand simulations, Γ decreased by 70 % level from 30 to 200 s, increased by 20 % level from 300 to 400 s, and then 50 % level from 500 to 600 s. Both case C and D successfully followed the slowly varying load in overall behavior. In this largely varying load simulation, case D exhibits a more desirable temperature profile than case C, characterized by reduced temperature variations where the thermal efficiency can be secured or enhanced. However, Case D necessitates active operations to counteract varying reactivity loss from drifting DNPs as shown in Fig. 15.

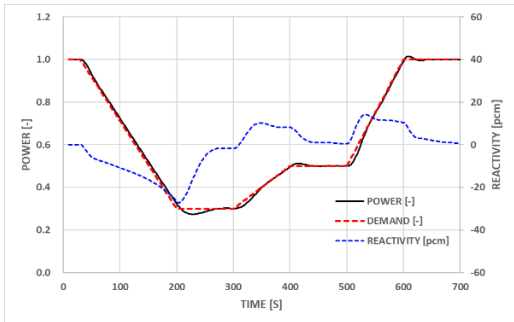


Fig. 10. Power profile with constant pump speed (C)

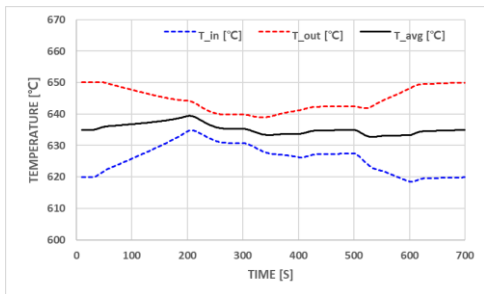


Fig. 11. Temperature profile with constant pump speed (C)

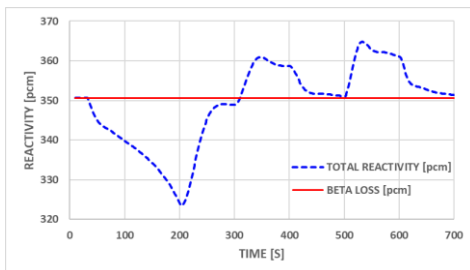


Fig. 12. Reactivity profile with constant pump speed (C)

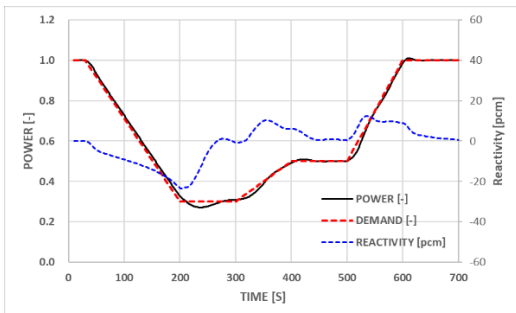


Fig. 13. Power profile with adaptive pump speed (D)

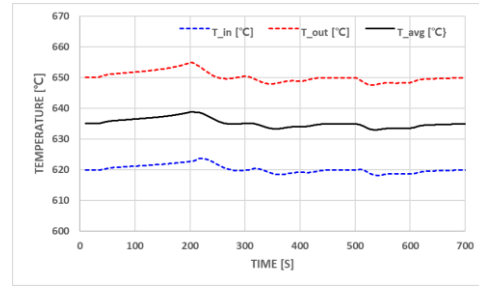


Fig. 14. Temperature profile with constant pump speed (D)

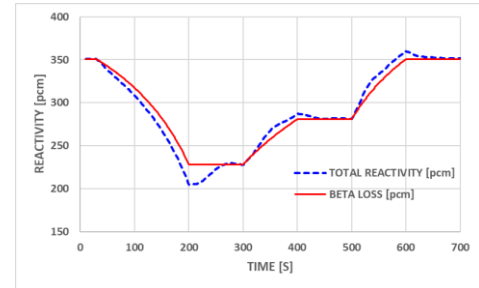


Fig. 15. Reactivity profile with constant pump speed (D)

4. Conclusions

Two cases of PLFO simulations with both constant and adaptive pump speeds demonstrated the Micro MSR's capability to effectively respond to dynamic power demand while accounting for the dynamic behavior of DNPs. However, despite the model's ability to capture the overarching dynamics of the circulating fuel system, there remains requirement for refinement.

These findings serve as preliminary data for improving more sophisticated PLFO simulation models. Further investigations, such as the fine mesh-wise velocity profile of fuel salt and analysis of temperature variations in the reflector, hold promise for refining the accuracy of local power profiles. It is expected that these enhancements will yield a comprehensive and precise PLFO simulation model, poised to meet the evolving demands for active contributions to electrical microgrids.

ACKNOWLEDGEMENT

This work was supported by Korea Research Institute for defense Technology planning and advancement (KRIT) grant funded by the Korea government (DAPA (Defense Acquisition Program Administration)) (KRIT-CT-22-017, Next Generation Multi-Purpose High Power Generation Technology (Liquid Fueled Heat Supply Module Design Technology), 2022).

REFERENCES

- [1] Kim, H., Kwon, C., Ham, S., Lee, J., Kim, S. J., & Kim, S. (2023). Physical properties of KCl-UC13 molten salts as potential fuels for molten salt reactors. *Journal of Nuclear Materials*, 577, 154329.
- [2] Guerrieri, C., Cammi, A., & Luzzi, L. (2013). An approach to the MSR dynamics and stability analysis. *Progress in Nuclear Energy*, 67, 56-73.